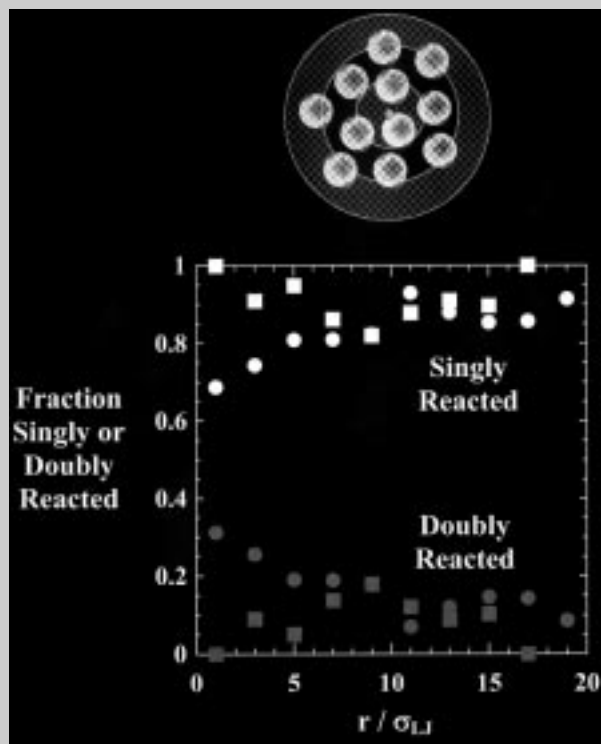


Full Paper: Radical homopolymerization of multifunctional monomers leads to highly crosslinked networks that demonstrate structural heterogeneity. Spatially non-uniform diffusion limitations result in complex reaction behavior such as unequal functional group reactivity, radical trapping, and microgel formation. The heterogeneity that arises in these systems on the molecular and nanoscopic scales is very difficult to characterize experimentally. A unique off-lattice simulation approach is described to provide insight into structural evolution during multifunctional monomer polymerizations. This simulation approach combines simple Monte Carlo principles to incorporate specie mobility with the basic reaction framework of traditional kinetic gelation models. Simulation volumes containing up to 100 000 Lennard–Jones spheres, representing tetrafunctional monomer units, were randomly configured with the Metropolis Method. Rules for initiation, propagation, and termination were developed and implemented, as well as local and periodic particle relaxation schemes. The simulation captures more realistic particle dynamics and mobility than traditional, lattice-based kinetic gelation models. In this work, a detailed description of the simulation method and selected results are presented. Agreement of simulated and experimental trends related to radical trapping frequency as a function of mobility is shown. Visual images of microgel evolution and simulated information about functional group reactivity within microgels are set forth.



Information within microgels is organized into concentric shells extending from the center of the microgel (top schematic). Of the monomer reacted into the network, the fractions that are singly (filled symbols) or doubly (open symbols) reacted are plotted versus distance from the center of reacted ends. The size of the reaction volume differs for the two series of data (circle: $r_{\text{rxn}} = 1.1 \sigma_{\text{LJ}}$, square: $r_{\text{rxn}} = 0.9 \sigma_{\text{LJ}}$). The system with the larger reaction volume has a higher fraction of doubly reacted monomer units located near the center of reactivity. The system with the smaller reaction volume has a more even distribution of doubly reacted units. The former system forms divinyl loops since a propagating radical can react with the pendant double bond from the same monomer. The latter system has a higher propensity to form longer singly reacted chains with less cyclization.

Off-Lattice Approach to Simulate Radical Chain Polymerizations of Tetrafunctional Monomers

J. Brian Hutchison,¹ Kristi S. Anseth*²

¹ Department of Chemical Engineering, University of Colorado, ECCH 111, Campus Box 424, Boulder, Colorado 80309-0424, USA

² Howard Hughes Medical Institute, University of Colorado, ECCH 111, Campus Box 424, Boulder, Colorado 80309-0424, USA
Fax: 303-492-4341; E-mail: Kristi.Anseth@Colorado.edu

Introduction

Highly crosslinked polymers synthesized by the chain polymerization of multifunctional monomers are desirable for a number of applications, including coatings,^[1] flexographic printing plates,^[2] dental restorative materi-

als,^[3] and future applications in biomedical and tissue engineered orthopedic materials.^[4] The physical and mechanical properties of highly crosslinked networks include low swelling and high moduli, both of which are desirable in many of the aforementioned applications.

While the structure of crosslinked networks imparts many desirable macroscopic properties, the evolution of the networks can be quite complex. Photoinitiated polymerizations of multifunctional monomers such as di(meth)acrylates exhibit fast polymerization rates at room temperature; however, these reactions exhibit numerous complexities related to the early onset of gelation.^[1] Researchers have shown an enhanced reactivity of pendant double bonds relative to monomeric double bonds in high crosslinking polymerizations, as well as changes in reactivity as a function of conversion.^[5–7] The pendant double bonds have an enhanced propensity for reaction because of their high local concentration at the site of the propagating radical.^[5] Unequal double bond reactivity and limited mobility of reacting species (e.g., trapped monomer and radicals) lead to a heterogeneous network structure that varies with conversion and over a range of size scales.^[5,7]

One important aspect of the network heterogeneity is the formation of microgel regions. Microgels, or nanoscopic areas of high intramolecular cycle or crosslink density, can influence the properties of highly crosslinked polymers on a macroscopic scale. In a comprehensive review of microgels, Funke et al.^[7] describe microgels as intramolecularly crosslinked macromolecules. This broad definition includes microgels made in emulsion and phase separated multiblock polymerizations, as well as homopolymerizations of multifunctional monomers. The microgels discussed and characterized in this work are those resulting from the chain homopolymerization of multifunctional monomers; in this context, microgels arise from reaction complexities. Indirect experimental observations of microgel formation have been published by a number of authors.^[1,6,7] In most examples, the evolution of microgels has been related to observations of enhanced pendant double bond reactivity.^[5]

Experimental methods to investigate molecular or nanoscopic polymerization events are difficult or impossible to employ for a number of reasons. For instance, the small size scale of interest and low conversion limit the variety of possible microscopic and spectroscopic techniques. In particular, nanoscale imaging techniques often require high vacuum and unnatural sample preparation. Furthermore, swelling of polymer regions with unreacted monomer results in indistinct boundaries between polymer and monomer. Although variations in density and refractive index are not observed, a few researchers have published direct experimental evidence of microgel formation.^[7,8] Nonetheless, simulations that realistically capture reaction events provide valuable insight into molecular and nanoscale phenomena. For instance, quantitative information about cyclization versus crosslinking has been described via simulations^[9–12] more often than by experiments.

Kinney and Scranton^[13] review three methods for modeling polymerizations of crosslinked networks. Statistical

and kinetic models, in addition to combinations of the two types of models, yield structural information such as gel and sol fractions, molecular weight between crosslinks, the number of elastically active chains, and polymerization rate behavior. However, these models are based on mean field averages of rate parameters and concentrations, so heterogeneity is not captured.

The third approach is a kinetic gelation simulation in which monomer units with a specific number of reactive ends are positioned at fixed points in a reaction volume. A specified fraction of reactive ends are “seeded” with active radicals, and these radicals propagate via a random walk through unreacted ends (unsaturated bonds). Termination of these active radicals occurs by combination with another radical (bimolecular termination) or propagation may cease when the local environment of the radical does not include any unreacted particle ends (radical trapping).

Manneville and de Seze^[14] developed the first kinetic gelation model, a percolation-type model, that was used to investigate critical exponents related to the statistical distribution of bonds between neighboring or second-neighboring monomer units. This type of simulation is limited to highly crosslinked polymerizations that are characterized by gelation at low conversion since individual species are fixed on a regular lattice array within the simulation box from the onset. The clear advantage of this type of simulation is the elimination of mean-field averages and the ability to capture polymerization heterogeneities to more realistically describe structural evolution. Conversely, designation of monomer units as fixed lattice points results in unrealistic representation of species dynamics and mobility at low conversion.

Early refinements to the kinetic gelation approach included the incorporation of void sites and exchange of void and monomer sites to represent mobility.^[15,16] Also, monomer molecules were created that occupy multiple lattice sites to investigate how monomer size affects network evolution.^[17] Bowman and Peppas introduced a two-site initiator specie and a decaying initiation scheme based on first order kinetics.^[17] Kinetic gelation simulations have been used to explore structural evolution with living radical initiation schemes as well.^[18] Anseth and Bowman explored copolymerization of multifunctional monomers, as well as cyclization and microgel formation.^[8,12] Finally, Boots et al. used an off-lattice variation of the classic kinetic gelation model to investigate network evolution in a liquid crystalline diacrylate monomer.^[19]

The example of an off-lattice model is a significant distinction from traditional kinetic gelation simulations. In the case of the liquid-crystal simulation, well-known energetic interactions and monomer geometry were incorporated along with rules for polymerization that evolved from the kinetic gelation simulations. This approach can

be extended to investigate monomers with undefined energetic and geometric characteristics. Conversely, one might imagine a molecular dynamics simulation that includes polymerization of monomer units.^[20] The use of molecular dynamics to dictate monomer mobility is well understood; however, the incorporation of reacting species in conjunction with a molecular dynamics simulation has not been widely explored. Simulations that combine mobility and particle interactions during polymerization reactions represent a separate class of models that, to this date, have not been fully developed.

Hence, this work aims to extend a traditional kinetic gelation model, specifically the off-lattice variation developed for liquid crystal systems, to more broadly capture the polymerization of various multifunctional monomers. In contrast to the conventional kinetic gelation model, this method is not restricted to reaction of monomer molecules fixed at lattice sites. Rather, monomer units move based on simple Monte Carlo principles. Using this approach, we aim to model molecular and nanoscale phenomena including radical trapping and unequal functional group reactivity that correspond to heterogeneous network evolution. Details of this unique simulation, including configuration of the simulation volume, polymerization rules, and relaxation or equilibration procedures, are described. Selected results that are complemented by experimental data are presented to validate the trends revealed by this model. Finally, results that cannot be collected with experiments, such as molecular network formation *within* microgels, are presented to illustrate the value of the simulation for gaining fundamental insight into crosslinking polymerization events.

The model presented herein is one of the first off-lattice simulations to examine chain crosslinking reactions of multifunctional monomers. While the present model uses a rather simple description for the particle energetics, the overall approach provides a convenient basis for the introduction of more complex extensions in many directions.

Simulation Development

Initial Configuration

A simple cubic array of spheres was created within a cubic volume with periodic boundary conditions. The simulation volume and the number of spheres in the volume were chosen to prevent unrealistic interaction of particles that travel farther than the box dimensions (i.e., through the periodic boundaries). A typical volume contained $\sim 10\,000$ to $\sim 100\,000$ particles that comprised 50% of the simulation space. Each sphere represented a single monomer unit with two reactive ends that were directly opposite of each other on the surface of the sphere. The diameter of the sphere (i.e., the distance between the

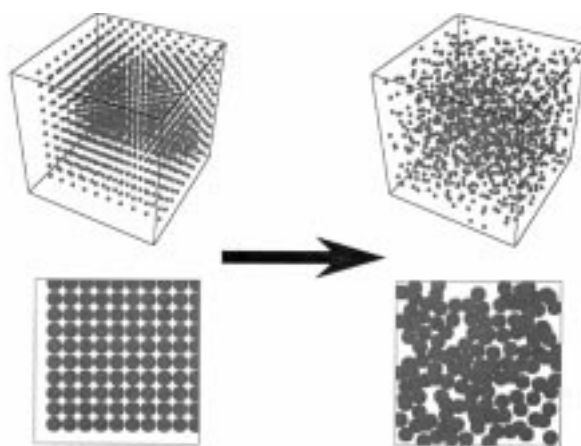


Figure 1. A simple cubic array of Lennard-Jones spheres (top, bottom left) is configured based on potential energy constraints and the Metropolis Criterion for move acceptance. Orientations of end functionality are randomized without regard to particle energetics.

reactive ends) is defined as σ_{LJ} . The subscript in this notation refers to the Lennard–Jones potential energy function that is used for particle dynamics calculations. Although this potential function allows for limited overlap of spheres, the distance between reacted ends is constant. The orientations of the spheres were randomized without consideration of energetics that may be specific to the reactive ends.

A simple Monte Carlo algorithm was used to dictate translational mobility of the particles. First, a move was proposed for a monomer particle. The total energy of the system was calculated for the particle in the new position based on a Lennard–Jones 6–12 potential function. The proposed move was either accepted or rejected based on the Metropolis Criterion.^[21] Specifically, if the system energy decreased due to the move, the move was accepted. Otherwise, a fraction of the energetically unfavorable moves were accepted based on a decaying exponential scale relative to the magnitude of the increase in total energy. The process of random particle selection and movement was repeated until particle positions in the box were completely randomized based on energetic constraints. Figure 1 depicts the initial configuration process of a box with 1 000 particles. A three-dimensional representation (top left) and a $\sim 1\sigma_{LJ}$ thick segment (bottom left) are shown before and after randomization. Before randomization, the simple cubic lattice arrangement of particles is evident. After randomization, the regular structure has disappeared (top and bottom right).

The initial randomization and configuration process was complete when the radial distribution plot of the monomer units took the form of a sub-critical liquid^[22] and stabilized. Also, the total potential energy of the system decreased to a minimum. Figure 2a reveals the radial distribution plot for a box containing 97 336 particles. The number density of particles, normalized by the average

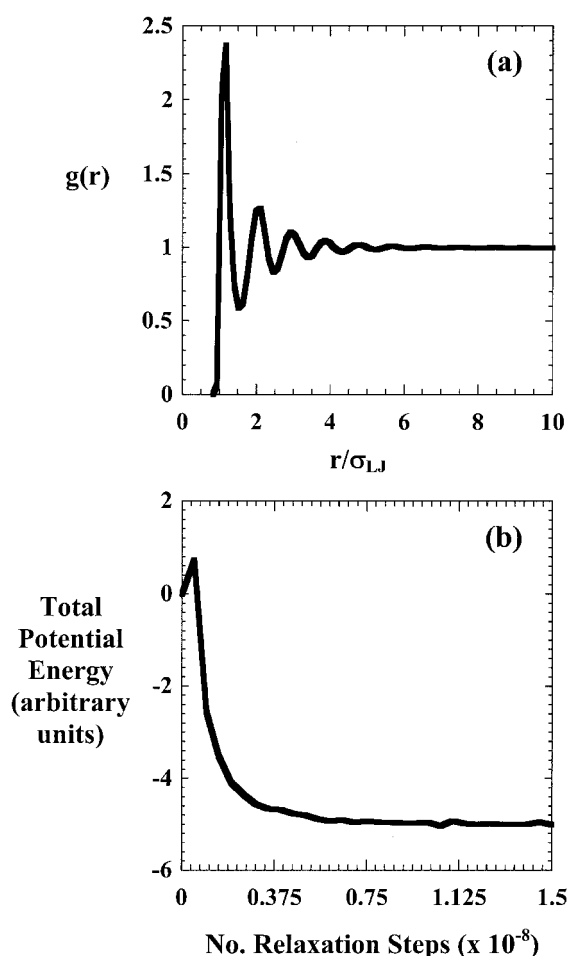


Figure 2. (a) The radial distribution plot of monomer molecules in the configured simulation box reveals a classic liquid-like form. Short-range order is evident and oscillatory decay results in convergence to the long-range particle density. (b) The total potential energy of the simulation volume decreases to a stable minimum. Minimization of the total potential energy and proper form of the radial distribution plot indicate that the simulation volume is randomly configured for polymerization.

particle number density, $g(r)$, is plotted as a function of radial distance from the center of each particle. The classic form for subcritical liquids is clear: short-range order is evident with long-range disorder that results from damped oscillatory behavior.^[22] The density of particles converges to the average particle density ($g(r) \rightarrow 1$). Furthermore, Figure 2b reveals the decrease in total potential energy in the system as a function of attempted relaxation steps. Minimization of the potential energy and stabilization of the radial distribution function indicate when the box is completely relaxed. Upon completion of this initial randomization, initiation of the polymerization commenced.

Initiation

A fraction of unreacted particle ends was designated as active sites (radicals). New active radicals were added

when propagating radicals became trapped. This initiation mechanism maintained a constant concentration of active radicals. Other initiation schemes could be incorporated in the simulation with very little difficulty. For example, decaying initiator concentrations and non-constant active radical concentrations may be more representative of certain polymerization conditions. Initiation via living radicals could be investigated by allowing reinitiation of bimolecularly-terminated radical species.

Propagation

Propagation occurred when an active radical end was linked to the nearest unreacted end within a defined reaction volume. A particle end containing a radical was selected randomly from the total number of propagating radicals. The size of a spherical reaction volume was defined for the entire simulation. Particles within the volume, centered on the selected radical, were identified to find the nearest unreacted particle end. Once found, the reacting end was linked to the neighboring end and the radical transferred to the new end. The size of the reaction volume is a parameter that is readily varied and represents a volume that each radical can sample during propagation events (i.e., a measure of local chain end mobility). For the results presented in this work, the radius of the reaction volume varied from $0.9\sigma_{LJ}$ to $1.1\sigma_{LJ}$. The kinetic chain, or sequence of reacted ends, for each radical, was stored as a linked list.^[21] Also, the reverse list was stored. The lists were updated after each successful reaction. These lists were used at different points during the simulation to extract information about the molecular structural evolution of the network (i.e., kinetic chain lengths, cyclization).

Figure 3 depicts polymerization within a box containing 9261 particles and ten active radicals. Figure 3a shows the initial positions of the particles with active ends in black. Figure 3b to 3d show the polymerization occurring from the initial radical sites. Singly reacted monomer particles are displayed in medium gray and doubly reacted particles are displayed in dark gray. Unreacted monomer particles are not shown; they are distributed throughout the remaining space of the simulation volume. Figure 3e reveals that a significant fraction of singly reacted monomer units is present throughout the box. Finally, Figure 3f shows a higher fraction of doubly reacted units.

Termination

The concentration of simulated active radicals shown in Figure 3 is higher than experimentally measured radical concentrations (10^{-10} – 10^{-3} M^[23]). This discrepancy was necessary to limit the number of monomer units in the simulation volume and the computation time. To prevent

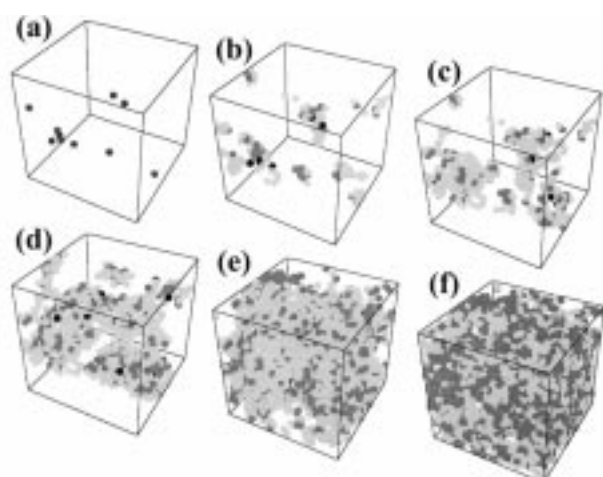


Figure 3. (a) 10 particle ends (in a box containing 9261 particles with 63% void space) are seeded with active radicals (black). (b–d) Radicals propagate to nearest unreacted particle ends. Doubly reacted particles are shown in dark gray; singly reacted units are medium gray. (e) A large fraction of the monomer units are singly reacted. (f) As conversion proceeds, more particles are doubly reacted and more radicals are trapped (shown in light gray). Unreacted particles are not shown; they fill the remainder of the occupied space in the box.

artificial interactions between active radicals, simulated termination proceeded via a radical trapping mechanism rather than bimolecular combination. When the local region of an active radical did not contain any unreacted particle ends, the reaction attempt was counted; the local environment was relaxed; but no propagation occurred. After fifty unsuccessful reaction attempts by an individual radical, the radical was considered trapped. This radical trapping mechanism was based on an assumption that the radical segment would not diffuse out of the local environment, and unreacted monomer would not travel into the region. Simulations indicated that radical propagation after fifty unsuccessful reaction attempts was very rare. Simulated radical trapping is depicted in Figure 4. In the left image, a radical is active (black) but surrounded by reacted monomer (medium and dark gray). The right image was captured after 100 reaction attempts among the ten active radicals (i.e., only a fraction of the reaction attempts was by the active radical discussed here). The same radical has become trapped (light gray) since no unreacted particle ends moved within the reaction volume of the active end. Radical trapping was the only mechanism allowed for termination in the simulation results presented. Other termination schemes, such as bimolecular termination, are easily incorporated.

Relaxation

A particularly important aspect of the simulation is the ability to incorporate more realistic mobility of reacting

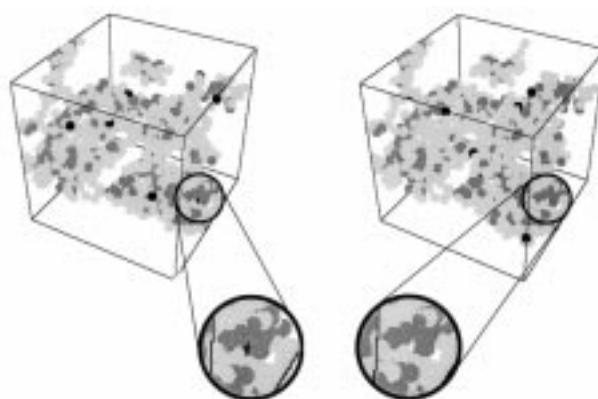


Figure 4. Termination of active radicals occurs by radical trapping. After 50 unsuccessful attempts at reaction with an unreacted particle end within a defined reaction volume, the radical becomes trapped (switches from black to light gray), and a new active end is introduced randomly to maintain a constant concentration of active radicals.

species compared to lattice-based simulations. The Monte Carlo methods used to configure the initial box before polymerization were also incorporated during the reaction process to maintain a minimized total potential energy throughout the simulation. After each propagation step, a local environment (different than the reaction volume) was relaxed. This local relaxation is a unique feature to the simulation. The simulation volume was divided into a number of equal size cells. Particles were assigned to a cell by implementing a linked list^[21] of the members of the cell. The local environment consisted of the cell containing the reacting particle as well as its 26 neighboring cells. The entire box was relaxed at designated points in the simulation as well. For the results in this work, global relaxation was completed after every 5% of the total propagation attempts. The number of relaxation steps executed between attempted reactions is another parameter that can be varied to simulate polymerizing monomers with different mobilities in the evolving network.

To summarize, the simulation was set up by randomizing and minimizing the total energy of a fixed number of unreacted particles. After the set-up, a fraction of monomer unit ends were initiated with active radicals. Each radical propagated to neighboring unreacted ends within a defined reaction volume according to specific polymerization rules. The local region surrounding the newly reacted particle was relaxed according to the Metropolis criteria. Propagation of the radicals proceeded until the active centers became trapped in local environments without unreacted ends; when trapping occurred, the trapped radicals were replaced with new active radicals to keep the overall active radical concentration constant. At regular intervals throughout the simulation, species throughout the entire box were relaxed and reconfigured based on the overall system energetics.

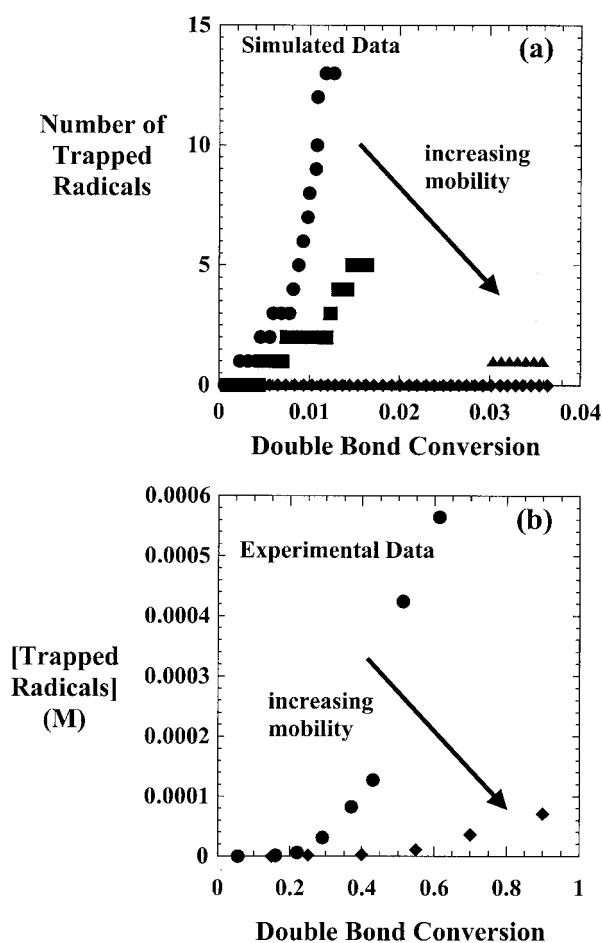


Figure 5. (a) Simulated data indicates a trend of decreasing frequency of radical trapping as mobility is increased by increasing the number of steps between attempted reactions and the size of the reaction volume. (circle: $n_{\text{steps}} = \text{low}$, $\text{vol}_{\text{rxn}} = \text{low}$; square: $n_{\text{steps}} = \text{high}$, $\text{vol}_{\text{rxn}} = \text{low}$; triangle: $n_{\text{steps}} = \text{low}$, $\text{vol}_{\text{rxn}} = \text{high}$; diamond: $n_{\text{steps}} = \text{high}$, $\text{vol}_{\text{rxn}} = \text{high}$) (b) The radical trapping rate is higher in the DEGDMA (circles) network, which is glassy (less mobility), compared to the PEG600DMA network (diamonds), which is rubbery (more mobility).

Results and Discussion

A classic feature of multifunctional monomer polymerizations is the development of microgels due to enhanced pendant double bond reactivity and localized mobility restrictions. The simulation described in this work is ideally suited to investigate phenomena that lead to heterogeneous structural evolution in highly crosslinked networks. Mobility of monomer specie and radical chain segments are two factors that affect the development of structure in crosslinked networks.

The number of relaxation steps between each propagation step represents monomer mobility in the system. Additionally, the volume that a propagating radical samples to locate an unreacted monomer end reflects segmental mobility. The effect of specie mobility on radical trapping is examined and compared to experimental data in

Figure 5. The two factors influencing mobility were investigated at two levels. The number of relaxation steps was increased by two orders of magnitude to simulate monomers with different mobilities. The radius of the reaction volume was increased from $0.9\sigma_{\text{LJ}}$ to $1.1\sigma_{\text{LJ}}$ to simulate increased mobility of the radical chain end.

Figure 5a depicts the simulated number of trapped radicals as a function of double bond conversion with varied specie mobility. A marked increase in the frequency of radical trapping is evident for the systems with lower mobility. Furthermore, the variation of the reaction volume size has a larger effect than varying the number of relaxation steps. Figure 5b shows experimental data, collected with electron paramagnetic resonance spectroscopy, of the concentration of trapped radicals as a function of double bond conversion in two different multifunctional monomer polymerizations: diethyleneglycol dimethacrylate (DEGDMA) and poly(ethylene glycol) ($\bar{M}_w = 600$) dimethacrylate (PEG600DMA).^[23] The trend in the experimental data is similar to the simulated data. The homopolymerization of DEGDMA, which reacts to form a glassy network at room temperature, creates a system with lower mobility than the homopolymerization of PEG600DMA, which forms a rubbery network at ambient conditions. Radical trapping occurs at a higher rate in the DEGDMA homopolymer than the PEG600DMA homopolymer.

While simulations are not quantitative in their predictions, they allow one to predict trends and test hypotheses related to effects of polymerization conditions on network formation. For example, quantitative comparison of simulated and experimental results in Figure 5 is not appropriate; however, the trends in data simulated at different mobility levels match corresponding experimental data. This agreement in trends is an important validation of the simulation results. The procedure used to collect the data in Figure 5b is relatively difficult and time consuming since each point represents a different experiment. Other experiments to investigate *molecular* network features are not possible due to the sampling volume of even the highest resolution spectroscopies.

The size scale of interest, which is much smaller than the sampling volume of any spectroscopic technique, is defined by the size of microgels that form ($<50 \text{ nm}$ ^[24]). Experimental images of microgels are difficult to obtain because electron microscopies require unnatural sample preparation and environmental conditions (i.e., heavy metal staining and high vacuum). However, pictures of microgel formation can be generated via simulation.

Figure 6 shows the evolution of a microgel simulated from a single activated particle end in a volume that contains 97336 particles with a 63% void fraction. Singly reacted monomer units are medium gray; doubly reacted units are dark gray; active radical ends are black; and trapped radicals are light gray. The unreacted units are

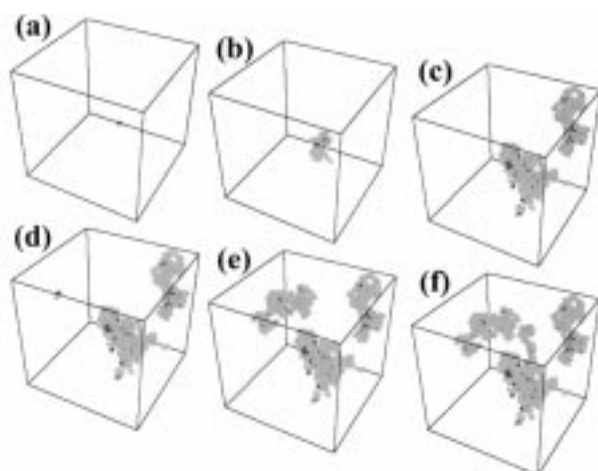


Figure 6. (a) A single active radical is placed in a box containing 97336 particles. (b–d) The radical propagates to form a microgel that appears as two structures due to polymerization through a periodic boundary. (d) The first radical becomes trapped and a new radical is added. (e–f) A second microgel forms and the radical traps.

not shown; they fill the space of the box not indicated by other colors. The first microgel grows until the propagating radical becomes trapped (a–c). The first microgel appears as two because it grows through the periodic boundaries. In fact, the microgel is a single interconnected unit that spans the simulation boundary. A second microgel grows to a terminal size (d–e), and finally the start of a third microgel between the first two is evident (e–f).

In addition to visual descriptions of microgels and their evolution, another particularly valuable aspect of the simulation described in this work is that it can provide useful information about molecular network formation *within* microgels that can not be investigated experimentally. For example, the fraction of doubly reacted monomer units can be found as a function of spatial position within the microgels. The location of the center of all reacted ends is more descriptive of the microgel geometry than the center of mass of all monomer units reacted into the microgel. The center of reactivity is designated as the center of mass of the reacted particles with doubly reacted particles weighted doubly (e.g., counted twice in the center of mass calculation). The location of the center of reactivity changes as the microgel evolves. A series of concentric spherical shells is centered on the calculated center of reactivity, which is shown as a two dimensional schematic in Figure 7 (top). The number of singly and doubly reacted units within each of these shells is counted. Figure 7 plots the fraction of reacted monomer that is doubly (open symbols) or singly (closed symbols) reacted, as a function of radial distance from the center of the microgel. The data was captured from simulations of a single microgel forming in a box containing 97336 particles with 50% void fraction. The size of the reaction

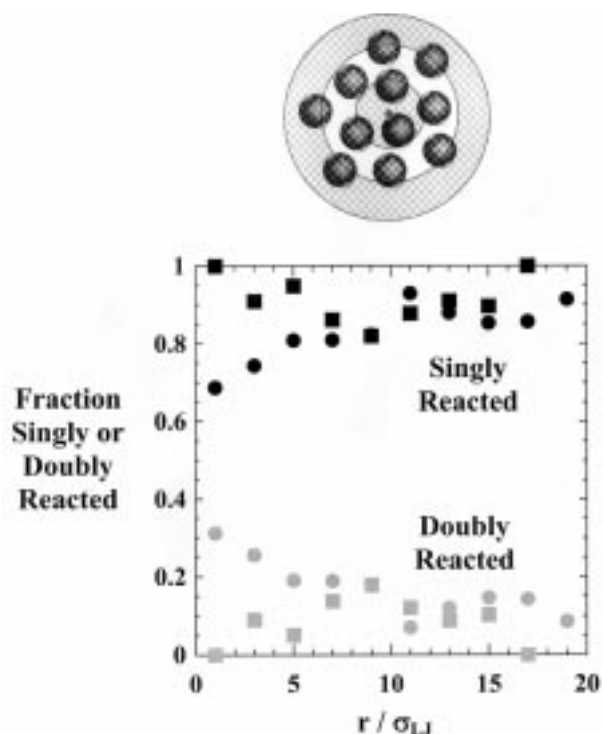


Figure 7. Information within microgels is organized into concentric shells extending from the center of the microgel (top schematic). Of the monomer reacted into the network, the fractions that are singly (black symbols) or doubly (gray symbols) reacted are plotted versus reaction distance from the center of reacted ends. The size of the reaction volume differs for the two series of data (circle: $r_{\text{rxn}} = 1.1\sigma_{\text{LJ}}$, square: $r_{\text{rxn}} = 0.9\sigma_{\text{LJ}}$). The system with the larger reaction volume has a higher fraction of doubly reacted monomer units located near the center of reactivity. The system with the smaller reaction volume has a more even distribution of doubly reacted units. The former system forms divinyl loops since a propagating radical can react with the pendant double bond from the same monomer. The latter system has a higher propensity to form longer singly reacted chains with less cyclization.

volume (i.e., the sphere centered on a propagating radical that encloses the collection of potential reaction partners) was varied. For the series of data displayed as squares, the maximum radial distance for reaction from a propagating radical is $0.9\sigma_{\text{LJ}}$. For the series shown as circles, the maximum reaction distance is $1.1\sigma_{\text{LJ}}$.

The system with a larger reaction volume forms more divinyl loops since a propagating radical can react with the opposite end of the same monomer unit. Conversely, the system with a smaller reaction volume has a higher propensity to form longer singly reacted chains. This difference is evident in Figure 7: the data that describe the system with a higher reaction volume have a higher fraction of doubly reacted units at the center of the microgel compared to the system with a shorter maximum reaction distance. Figure 7 provides a simple example of the information that can be obtained from this simulation to provide a molecular and structural description of highly

crosslinked polymers. In the case of the pendant double bond reactivity response in Figure 7, the result (that a larger reaction volume leads to a more highly crosslinked microgel core) was observed for a number of independent pairs of runs in which the reaction volume was changed from $0.9\sigma_{LJ}$ to $1.1\sigma_{LJ}$.

The simulation described in this work is ideally suited for an investigation into the geometric and conversion-based evolution of microgels for systems of varied mobility. In addition, variations of monomer functionality and distribution of reactive ends on the monomer sphere will provide important insight to further improve the design of multifunctional monomer systems and better understand heterogeneities that arise in chain crosslinking polymerizations.

Conclusions

An off-lattice variation of a kinetic gelation model was developed that incorporates simple Monte Carlo principles to impart more realistic monomer mobility. In addition, specific rules for polymerization, including initiation, propagation, and radical trapping, are implemented to simulate homopolymerization of a divinyl monomer. This approach is important for describing network formation in high-crosslinking chain polymerizations. Simulated results are in qualitative agreement with experimental data such as radical trapping frequency as a function of system mobility. Agreement with specific experimental data leads to the confirmation that the simulation can accurately describe trends that are difficult to observe experimentally. For example, visual images of microgel evolution are shown. In addition, simulated results are presented for molecular evolution (i.e., pendant double bond reactivity) *within* microgels.

Acknowledgement: The authors gratefully acknowledge the American Chemical Society Petroleum Research Fund (32850-G7), the NSF Graduate Research Fellowship Program (JBH), and the NSF IUCRC for Fundamentals and Applications of Photopolymerizations.

Received: January 19, 2001

Revised: April 30, 2001

- [1] J. G. Kloosterboer, *Adv. Polym. Sci.* **1988**, *84*, 1.
- [2] C. Decker, *Acta Polym.* **1994**, *45*, 333.
- [3] K. S. Anseth, S. M. Newman, C. N. Bowman, "Polymeric Dental Composites: Properties and Reaction Behavior of Multimethacrylate Dental Restorations", in: *Biopolymers II*, Springer, Berlin 1995, Vol. 122, p. 177.
- [4] D. S. Muggli, A. K. Burkoth, S. A. Keyser, H. R. Lee, K. S. Anseth, *Macromolecules* **1998**, *31*, 4120.
- [5] J. G. Kloosterboer, G. M. M. van de Hei, H. M. J. Boots, *Polym. Commun.* **1984**, *25*, 354.
- [6] H. M. J. Boots, J. G. Kloosterboer, G. M. M. van de Hei, R. B. Pandey, *Br. Polym. J.* **1985**, *17*, 219.
- [7] W. Funke, O. Okay, B. Joos-Muller, "Microgels – Intramolecularly Crosslinked Macromolecules with a Globular Structure", in: *Microencapsulation – Microgels – Iniferters*, Springer, Berlin 1998, Vol. 136, p. 139.
- [8] K. S. Anseth, C. N. Bowman, *J. Polym. Sci., Part B: Polym. Phys.* **1995**, *33*, 1769.
- [9] I. I. Romantsova, *Int. J. Polym. Mater.* **1993**, *19*, 51.
- [10] R. Hendrickson, A. Gupta, C. W. Macosko, *Comput. Polym. Sci.* **1995**, *5*, 135.
- [11] K. Dusek, J. Somvarsky, *Polym. Int.* **1997**, *44*, 225.
- [12] K. S. Anseth, C. N. Bowman, *Chem. Eng. Sci.* **1994**, *49*, 2207.
- [13] A. B. Kinney, A. B. Scranton, "Formation and Structure of Cross-Linked Polyacrylates – Methods For Modeling Network Formation", in: *Superabsorbent Polymers*, American Chemical Society, Washington 1994, Vol. 573, p. 2.
- [14] P. Manneville, L. de Seze, "Percolation and Addition by Additive Polymerization", in: *Numerical Methods in the Study of Critical Phenomena*, J. Della Dora, J. Demongeot, B. Lacolle, Eds., Springer, Berlin 1981, p. 116.
- [15] H. J. Herrmann, D. P. Landau, D. Stauffer, *Phys. Rev. Lett.* **1982**, *49*, 412.
- [16] R. Bansil, H. J. Herrmann, D. Stauffer, *Macromolecules* **1984**, *17*, 998.
- [17] C. N. Bowman, N. A. Peppas, *Chem. Eng. Sci.* **1992**, *47*, 1411.
- [18] J. H. Ward, N. A. Peppas, *Macromolecules* **2000**, *33*, 5137.
- [19] H. M. J. Boots, K. S. Anseth, D. L. Kurdikar, N. A. Peppas, "Network Formation by Chain Polymerization of a Liquid Crystalline Monomer", in: *The Wiley Polymer Networks Group Review Series*, K. te Nijenhuis, W. J. Mijs, Eds., John Wiley & Sons, New York 1998, Vol. 1, p. 377.
- [20] D. C. Doherty, B. N. Holmes, P. Leung, R. B. Ross, *Comput. Theor. Polym. Sci.* **1998**, *8*, 169.
- [21] M. P. Allen, D. L. Tildesley, "Computer Simulation of Liquids", Clarendon Press, Oxford 1987.
- [22] J. W. Tester, M. Modell, "Thermodynamics and Its Applications", 3rd edition, Prentice Hall PTR, Upper Saddle River 1997.
- [23] K. S. Anseth, K. J. Anderson, C. N. Bowman, *Macromol. Chem. Phys.* **1996**, *197*, 833.
- [24] J. B. Hutchison, K. S. Anseth, unpublished data.